Atmos. Chem. Phys. Discuss., https://doi.org/10.5194/acp-2017-636
Manuscript under review for journal Atmos. Chem. Phys.
Discussion started: 8 August 2017

Atmospheric Chemistry and Physics Discussions

New particle formation in the sulfuric acid-dimethylamine-water system: Reevaluation of CLOUD chamber measurements and comparison to an aerosol nucleation and growth model

Andreas Kürten[1], Chenxi Li[2], Federico Bianchi[3], Joachim Curtius[1], António Dias[4], Neil M. Donahue[5], Jonathan Duplissy[3], Richard C. Flagan[6], Jani Hakala[3], Tuija Jokinen[3], Jasper Kirkby[1,7], Markku Kulmala[3], Ari Laaksonen[8], Katrianne Lehtipalo[3,9], Vladimir Makhmutov[10], Antti Onnela[7], Matti P. Rissanen[3], Mario Simon[1], Mikko Sipilä[3], Yuri Stozhkov[10], Jasmin Tröstl[9], Penglin Ye[5,11], and Peter H. McMurry[2]

[1]Institute for Atmospheric and Environmental Sciences, Goethe University Frankfurt, 60438 Frankfurt am Main, Germany.
[2]Department of Mechanical Engineering, University of Minnesota, 111 Church St. SE, Minneapolis, MN 55455, USA.
[3]Department of Physics, University of Helsinki, FI-00014 Helsinki, Finland.
[4]SIM, University of Lisbon, 1849-016 Lisbon, Portugal.
[5]Center for Atmospheric Particle Studies, Carnegie Mellon University, Pittsburgh, Pennsylvania 15213, USA.
[6]Division of Chemistry and Chemical Engineering, California Institute of Technology, Pasadena, California 91125, USA.
[7]CERN, CH-1211 Geneva, Switzerland.
[8]Finnish Meteorological Institute, FI-00101 Helsinki, Finland.
[9]Laboratory of Atmospheric Chemistry, Paul Scherrer Institute, 5232 Villigen PSI, Switzerland.
[10]Solar and Cosmic Ray Research Laboratory, Lebedev Physical Institute, 119991 Moscow, Russia.
[11]Aerodyne Research Inc., Billerica, Massachusetts 01821, USA.

Correspondence to: Andreas Kürten (kuerten@iau.uni-frankfurt.de)

Atmos. Chem. Phys. Discuss., https://doi.org/10.5194/acp-2017-636
Manuscript under review for journal Atmos. Chem. Phys.
Discussion started: 8 August 2017

Atmospheric Chemistry and Physics Discussions

Abstract

A recent CLOUD (Cosmics Leaving OUtdoor Droplets) chamber study showed that sulfuric acid and dimethylamine produce new aerosols very efficiently, and yield particle formation rates that are compatible with boundary layer observations. These previously published new particle formation (NPF) rates are re-analyzed in the present study with an advanced method. The results show that the NPF rates at 1.7 nm are more than a factor of 10 faster than previously published due to earlier approximations in correcting particle measurements made at larger detection threshold. The revised NPF rates agree almost perfectly with calculated rates from a kinetic aerosol model at different sizes (1.7 nm and 4.3 nm mobility diameter). In addition, modeled and measured size distributions show good agreement over a wide range (up to ca. 30 nm). Furthermore, the aerosol model is modified such that evaporation rates for some clusters can be taken into account; these evaporation rates were previously published from a flow tube study. Using this model, the findings from the present study and the flow tube experiment can be brought into good agreement. This confirms that nucleation proceeds at rates that are compatible with collision-controlled (a.k.a. kinetically-controlled) new particle formation for the conditions during the CLOUD7 experiment (278 K, 38% RH, sulfuric acid concentration between 1×10^6 and 3×10^7 cm^{-3} and dimethylamine mixing ratio of ~40 pptv). Finally, the simulation of atmospheric new particle formation reveals that even tiny mixing ratios of dimethylamine (0.1 pptv) yield NPF rates that could explain significant boundary layer particle formation. This highlights the need for improved speciation and quantification techniques for atmospheric gas-phase amine measurements.

Atmos. Chem. Phys. Discuss., https://doi.org/10.5194/acp-2017-636
Manuscript under review for journal Atmos. Chem. Phys.
Discussion started: 8 August 2017

Atmospheric Chemistry and Physics Discussions

1. INTRODUCTION

The formation of new particles by gas-to-particle conversion (nucleation or new particle formation, NPF) is important for a variety of atmospheric processes and for human health.

It has been shown in numerous studies that sulfuric acid (H_2SO_4) is often associated with NPF (Weber et al., 1997; Kulmala et al., 2004; Fiedler et al., 2005; Kuang et al., 2008; Kirkby et al., 2011) and indeed it can explain some of the observed particle formation together with water vapor for neutral (uncharged) and ion-induced conditions when temperatures are low, e.g., in the free troposphere (Lee et al., 2003; Lovejoy et al., 2004; Duplissy et al., 2016; Ehrhart et al., 2016; Dunne et al., 2016). However, at least one additional stabilizing compound is required in order to explain boundary layer nucleation at warm temperatures. Acid-base nucleation, which involves a ternary compound, e.g., ammonia, besides sulfuric acid and water, can lead to much higher NPF rates compared to the binary system (Weber et al., 1998; Ball et al., 1999; Kürten et al., 2016a). Nevertheless, for most conditions close to the surface, the concentrations of H_2SO_4 and NH_3 are too low, or temperatures are too high, to allow significant ternary nucleation of these compounds (Kirkby et al., 2011; Kürten et al., 2016a). However, the substitution of ammonia by amines, e.g., dimethylamine ($(CH_3)_2NH$), leads to NPF rates that can explain the atmospheric observations over a wide range of sulfuric acid concentrations, even when the amine mixing ratios are in the low pptv-range (Kurtén et al., 2008; Nadykto et al., 2011; Ortega et al., 2012; Chen et al., 2012; Almeida et al., 2013; Glasoe et al., 2015). A recent study even showed that NPF is collision-controlled, i.e., that it proceeds at the maximum possible speed (Rao and McMurry, 1989), when amine mixing ratios are above ~20 pptv, and sulfuric acid concentrations are between 1×10^6 cm^{-3} and 3×10^7 cm^{-3} at 278 K and 38% RH (Kürten et al., 2014). Indications that NPF can be collision-limited were reported more than 30 years ago based on the analysis of chamber nucleation experiments (McMurry, 1980), although the involvement of amines, which were probably present as a contaminant during those experiments, was not considered. Indications that atmospheric nucleation might occur by a collision-limited process have also been previously presented (Weber et al., 1996). Despite the strong evidence that sulfuric acid-amine nucleation is very efficient, it has rarely been observed in the atmosphere. Only one study has so far reported sulfuric acid-amine nucleation (Zhao et al., 2011) despite amine mixing ratios of up to tens of pptv at some sites (Freshour et al., 2014; Yao et al., 2016). A global modelling study of sulfuric acid-amine nucleation has been carried out so far (Bergman et al., 2015) applying a nucleation parametrization based on the measurements of Almeida et al. (2013) and Glasoe et al. (2015).

Atmospheric boundary layer nucleation can also be explained by the existence of highly-oxygenated organic molecules (Crounse et al., 2013; Ehn et al., 2014), e.g., from α-pinene. These highly-oxygenated molecules have been found to nucleate efficiently even without the involvement of sulfuric acid, especially when ions take part in the nucleation process (Kirkby et al., 2016).

Even though oxidized organics seem to be globally important for NPF (Jokinen et al., 2015; Gordon et al., 2016; Dunne et al., 2016), the formation of new particles by sulfuric acid and amines should still be considered because sulfuric acid-amine nucleation rates exceed those from oxidized organics as soon as the concentrations of the precursor gases (sulfuric acid and

amines) are high enough (Berndt et al., 2014). Therefore, at least locally or regionally, i.e., close to sources, amines should be relevant.

In this study, we reanalyze data from the CLOUD7 campaign (during October/November 2012, see Almeida et al., 2013; Kürten et al., 2014), using an advanced method that takes into account the effect of self-coagulation in the estimation of new particle formation rates (Kürten et al., 2015a). These re-analyzed data and NPF rates obtained from Scanning Mobility Particle Sizer (SMPS) measurements are compared to results from a kinetic aerosol model. Modeling is also used for a comparison between a flow tube study (Jen et al., 2016a) and the CLOUD results, and for comparison to atmospheric boundary layer new particle formation rates.

2. METHODS

2.1 CLOUD experiment and instruments

The CLOUD (Cosmics Leaving OUtdoor Droplets) experiment at CERN was designed to investigate nucleation and growth of aerosol particles in chemically diverse systems. Additionally, the influence of ions on new particle formation (NPF) and growth can be studied inside the 26.1 m^3 electro-polished stainless steel chamber (Kirkby et al., 2011). For the experiments discussed in this paper, NPF is initiated by illuminating the air inside the chamber with UV light by means of a fiber-optic system (Kupc et al., 2011), which produces sulfuric acid (H_2SO_4) photolytically from reactions involving O_3, H_2O, SO_2 and O_2. Diluted dimethylamine and sulfur dioxide are taken from gas bottles; inside the chamber, these trace gases mix with clean synthetic air (i.e., O_2 and N_2 with a ratio of 21:79 from evaporated cryogenic liquids). To ensure homogenous conditions, the air is mixed with magnetically driven fans installed at the top and bottom of the chamber (Voigtländer et al., 2012). A thermal housing controls the chamber temperature to 278.15 K within several hundredths of a degree. The temperature was not varied for the experiments relevant for this study. The relative humidity was kept constant at 38% by humidifying a fraction of the inflowing air with a humidification system (Duplissy et al., 2016). In order to keep the pressure inside the chamber at 1.005 bar, the air that is taken by the instruments has to be continuously replenished. Therefore, a flow of 150 l/min of the humidified air is continuously supplied to the chamber. For the sulfuric acid, dimethylamine and water system, ions do not have a strong enhancing effect on the nucleation rates for most conditions (Almeida et al., 2013); therefore, we do not distinguish between the neutral and charged pathway in such runs.

A suite of instruments is connected to the CLOUD chamber to measure particles, ions, clusters and gas concentrations. A summary of these instruments is provided elsewhere (Kirkby et al., 2011; Duplissy et al., 2016). For this study, measured sulfuric acid and particle concentrations are relevant. A Chemical Ionization-Atmospheric Pressure interface-Time Of Flight Mass Spectrometer (CI-APi-TOF) was employed to measure sulfuric acid and its neutral clusters in this study (Jokinen et al., 2012; Kürten et al., 2014). The particle concentrations originate from a scanning mobility particle sizer (Wang and Flagan, 1990), which measured the particle size distribution between ~4 and ~80 nm. The mixing ratio of dimethylamine was determined by ion chromatography (Praplan et al., 2012; Simon et al., 2016).

Atmos. Chem. Phys. Discuss., https://doi.org/10.5194/acp-2017-636
Manuscript under review for journal Atmos. Chem. Phys.
Discussion started: 8 August 2017

Atmospheric Chemistry and Physics Discussions

2.2 Calculation of particle formation rates

Particle formation rates J (cm^{-3} s^{-1}) are calculated from the measured size distributions (assumed to consist of n bins). For the size bin with the index m, the rate at which particles with a diameter equal or larger than d_m are formed can be calculated according to (Kürten et al., 2015a):

$$J_{\geq m} = \frac{dN_{\geq m}}{dt} + \sum_{i=m}^{n}\left(k_{w,i} \cdot N_i\right) + k_{dil} \cdot N_{\geq m} + \sum_{i=m}^{n}\left(\sum_{j=i}^{n} s_{i,j} \cdot K_{i,j} \cdot N_j \cdot N_i\right). \quad (1)$$

This equation takes into account the time-rate-of-change of the number density of all particles for which $d_p \geq d_m$, i.e., $N_{\geq m}$, and corrects for the effects of wall loss (size dependent wall loss rates $k_{w,i}$), dilution (dilution rate k_{dil}), and coagulation (collision frequency function $K_{i,j}$), where N_i and N_j are the particle number densities in different size bins. The rate of losses to the chamber walls can be expressed by (Crump and Seinfeld, 1981):

$$k_w\left(d_p\right) = C_w \cdot \sqrt{D\left(d_p\right)}, \quad (2)$$

where $D(d_p)$ is the diffusivity of a particle of diameter d_p, which is given by the Stokes-Einstein relation (Hinds, 1999),

$$D\left(d_p\right) = \frac{k_B \cdot T \cdot C_C}{3 \cdot \pi \cdot \eta \cdot d_p}, \quad (3)$$

where k_b, T, η, are the Boltzmann constant, the temperature, and the gas viscosity, respectively. The Cunningham slip correction factor, C_C, is a function of the particle Knudsen number, $Kn = 2\lambda/d_p$, and λ is the mean-free-path of the gas molecules. The empirically derived proportionality coefficient, C_w, depends upon the chamber dimensions and on the intensity of turbulent mixing. The rate of loss of sulfuric acid to the chamber walls is generally used to characterize C_w. The diffusivity of sulfuric acid is 0.0732 cm^2 s^{-1} at 278 K and 38% RH (Hanson and Eisele, 2000). The measured life time, determined from the decay of sulfuric acid when the UV light is turned off, was 554 s (wall loss rate 0.00181 s^{-1}), with the experimentally determined diffusivity this yields a factor C_w of 0.00667 cm^{-1} $s^{-0.5}$. However, in this study diffusivities were calculated according to equation (3), so the calculated monomer diffusivity (for a monomer with a density of 1470 kg m^{-3} and a molecular weight of 0.143 kg mol^{-1}, see section 2.4) required a different scaling, resulting in a value of C_w = 0.00542 cm^{-1} $s^{-0.5}$ that was used throughout this study.

Dilution is taken into account by a loss rate that is independent of size and equals k_{dil} = 9.6×10^{-5} s^{-1}. Correcting for particle-particle collisions requires the calculation of the collision frequency function. We used the method from Chan and Mozurkewich (2001). This method includes the effect of enhanced collision rates through van der Waals forces. A value of 6.4×10^{-20} J was used for the Hamaker constant (Hamaker, 1937), leading to a maximum enhancement factor of ~2.3 for the smallest clusters, relative to the collision rate in the absence of van der Waals forces. The factor of 2.3 has previously been shown to give good agreement between measured and modeled cluster and particle concentrations for the chemical system of

sulfuric acid and dimethylamine (Kürten et al., 2014; Lehtipalo et al., 2016). In order to consider the collisions of particles in the same size bin, a scaling factor $s_{i,j}$ is used in equation (1), which is 0.5 when $i = j$ and 1 otherwise.

2.3 Reconstruction method

Recently a new method was introduced, that makes it possible to retrieve new particle formation rates at sizes below the threshold of the instrument used to determine the particle number density. This method is capable of considering the effect of self-coagulation (Kürten et al., 2015a). It requires introducing new size bins below the threshold of the SMPS (termed d_{p2} in the following; d_{p2} corresponds to the index $m = 1$). The method starts by calculating the number density in the first newly introduced smaller size bin (index $m = 0$, diameter d_{p2} - dd_p):

$$N_{m-1} = \left(d_{p,m} - d_{p,m-1}\right) \cdot \frac{J_{\geq m}}{GR_{m-1}} \approx \mathrm{d}d_p \cdot \frac{J_{\geq m}}{GR}. \quad (4)$$

Here, the particle growth rate GR (nm s^{-1}) needs to be used as well as the difference between two adjacent size bins (dd_p). Once the number density in the newly introduced bin is known this information can be used to calculate J_{m-1}. In the further steps, the numbers N_{m-2} and J_{m-2} are calculated and so on. In this way, the size distribution can be extrapolated towards smaller and smaller sizes in a stepwise process until eventually reaching the diameter d_{p1}.

The method has so far only been tested against simulated data but not against measured size distributions (Kürten et al., 2015a). In this study the smallest measured SMPS diameter is d_{p2} = 4.3 nm; 26 new size bins with dd_p = 0.1 nm were introduced and this enabled the calculation of the NPF rates at d_{p1} = 1.7 nm in the smallest size bin. This size was chosen since previously published particle formation rates from the CLOUD experiment were reported for this diameter (e.g. Kirkby et al., 2011; Almeida et al., 2013; Riccobono et al., 2014).

2.4 Kinetic new particle formation and growth model

The measured particle formation rates are compared to modeled formation rates assuming collision-limited particle formation, i.e., all clusters are not allowed to evaporate. McMurry (1980) was the first to show that number concentrations and size distributions of particles formed photochemically from SO_2 in chamber experiments (Clark and Whitby, 1975) are consistent with collision-controlled nucleation; results from updated versions of this model have recently been presented (Kürten et al., 2014; McMurry and Li, 2017). The model used here has been described previously (Kürten et al., 2014; Kürten et al., 2015a, Kürten et al. 2015b) but only brief introductions were reported; therefore, more details are provided in the following.

As outlined in Kürten et al. (2014), collision-controlled new particle formation accurately described the measured cluster distributions for the sulfuric acid-dimethylamine system up to the pentamer (cluster containing five sulfuric acid molecules). In this model, it was assumed that the clusters consist of “monomeric” building blocks, each containing one sulfuric acid and one dimethylamine molecule. Evidence that this 1:1-ratio between acid and base is approximately maintained for the small clusters was presented from neutral and charged cluster

measurements (Almeida et al., 2013; Kürten et al., 2014; Bianchi et al., 2014; Glasoe et al., 2015). The molecular weight was, therefore, chosen as 0.143 kg mol^{-1} (sum of sulfuric acid with 0.098 kg mol^{-1} and dimethylamine with 0.045 kg mol^{-1}), and the density as 1470 kg m^{-3} (Qiu and Zhang, 2012).

During the reported experiments (CLOUD7 in fall 2012), dimethylamine was always present at mixing ratios above ca. 20 pptv. Dimethylamine (DMA) was supplied from a certified gas bottle and diluted with synthetic air before it was introduced into the chamber to achieve the desired mixing ratios. Sulfuric acid was generated in situ from the reactions between SO_2 and OH whenever the UV light was turned on (see section 2.1). Since the UV light intensity and the gas concentrations were kept constant throughout each individual experiment, it is justified to assume a constant monomer production rate P_1. The equation describing the temporal development of the monomer concentration, N_1, is

$$\frac{dN_1}{dt} = P_1 - \left(k_{1,w} + k_{dil} + \sum_{j=1}^{N_{max}} K_{1,j} \cdot N_j\right) \cdot N_1 \quad (5)$$

and, for the clusters containing two or more sulfuric acid molecules ($k \geq 2$),

$$\frac{dN_k}{dt} = \frac{1}{2} \cdot \sum_{i+j=k} K_{i,j} \cdot N_i \cdot N_j - \left(k_{w,k} + k_{dil} + \sum_{j=1}^{N} K_{k,j} \cdot N_j\right) \cdot N_k. \quad (6)$$

The same loss mechanisms (wall loss, dilution and coagulation) as for the calculation of the particle formation rates (section 2.2) are considered when modeling the cluster concentrations. In this study, the particle size distribution was calculated from the monomer up to a diameter of ~84 nm, which corresponds to the upper size limit of the SMPS used in CLOUD7. Tracking each individual cluster/particle up to this large size would be computationally too demanding, so the size distribution was divided into so-called molecular size bins (tracking each individual cluster), and geometric size bins, where the mid-point diameters of two neighboring size bins differ by a constant factor. The number of molecular size bins was set to 400 (which results in a diameter of ~5 nm for the largest molecular bin), while the number of geometric size bins was set to 190 with a geometric factor of 1.015 (maximum diameter of the last bin is 83.7 nm). The treatment of the geometric size bins was similar to the molecular bins, except that the collision products were distributed between the two closest size bins. Two smaller particles with diameters $d_{p,i}$ and $d_{p,j}$ generate a cluster with size

$$d_{p,x} = \left(d_{p,i}^3 + d_{p,j}^3\right)^{1/3}. \quad (7)$$

If it is assumed that the collision product falls into the size range covered by the geometric bins, its diameter will be between two size bins $d_{p,k}$ and $d_{p,k+1}$. The production rate of particles with diameter $d_{p,x}$ is

$$P_x = s_{i,j} \cdot K_{i,j} \cdot N_i \cdot N_j. \quad (8)$$

The resulting particles are distributed between the two bins to conserve mass, i.e.,

Atmos. Chem. Phys. Discuss., https://doi.org/10.5194/acp-2017-636
Manuscript under review for journal Atmos. Chem. Phys.
Discussion started: 8 August 2017

Atmospheric Chemistry and Physics Discussions

$$P_k = \left(\frac{d_{p,k+1}^3 - d_{p,x}^3}{d_{p,k+1}^3 - d_{p,k}^3}\right) \cdot P_x, \quad (9a)$$

$$P_{k+1} = \left(1 - \frac{d_{p,k+1}^3 - d_{p,x}^3}{d_{p,k+1}^3 - d_{p,k}^3}\right) \cdot P_x. \quad (9b)$$

The first terms on the right hand side of equations (9a) and (9b) determine the fraction by how much the diameter of the newly-formed particle can be associated with either of the two neighboring bins. The second factor accounts for the fact that the total mass of the newly-formed particles needs to be conserved, therefore, a scaling with the particle diameters to the power of three is necessary. When the collision product falls into the molecular size bin regime the calculation is straightforward because the diameter of the product agrees exactly with a molecular bin and does not need to be distributed between two bins (see the production term in equation (6)). In case the collision products exceed the largest bin diameter, the product is entirely assigned to the largest bin, while taking into account the scaling such that the total mass is conserved.

In the model, no free parameter is used as the concentration of monomers is constrained by the measurements. Therefore, the production rate P_1 is adjusted such that the resulting monomer concentration in the model matches the measured sulfuric acid concentration. The model is used to simulate the experiments for a duration of 10,000 s with a time resolution of 1 s. For the small clusters and particles this leads to a steady-state between production and loss; therefore, the resulting concentrations are essentially time-independent.

The model introduced here was compared with the model described in McMurry and Li (2017) and yielded almost indistinguishable results for several scenarios when the same input parameters were used. We take this as an indication that both models correctly describe collision-controlled nucleation, especially since the models were independently developed and do not share the same code. The model in this paper is based on defining size bins according to their diameter, while the model by McMurry and Li (2017) uses particle volume.

3. RESULTS

3.1 Comparison between Almeida et al. (2013) and SMPS derived NPF rates

Using the model described in section 2.4, a comparison between the previously published NPF rates from Almeida et al. (2013) and the modeled rates was performed. Almeida et al. (2013) derived NPF rates for a particle mobility diameter of 1.7 nm. Using a density of 1470 kg m^{-3} and a molecular weight of 0.143 kg mol^{-1}, it can be calculated that a spherical cluster containing nine monomers (nonamer) has a geometric diameter of ~1.4 nm, i.e., a mobility diameter of 1.7 nm (Ku and Fernandez de la Mora, 2009); therefore, the modeled nonamer formation rates were used for the comparison.

Figure 1 shows the modeled formation rates at 1.7 nm and the Almeida et al. (2013) data as a function of the sulfuric acid concentration (which is equivalent to the monomer concentration in the model, see section 2.4, since it is assumed that all sulfuric acid is bound to DMA). It can be seen that the modeled NPF rates are significantly higher. This indicates that the previously

Atmos. Chem. Phys. Discuss., https://doi.org/10.5194/acp-2017-636
Manuscript under review for journal Atmos. Chem. Phys.
Discussion started: 8 August 2017

Atmospheric Chemistry and Physics Discussions

published formation rates underestimate the true formation rates if sulfuric acid-dimethylamine nucleation is indeed proceeding at the collision-limit. Previously published results indicated that this is the case (Kürten et al., 2014; Lehtipalo et al., 2016); however, we will provide further evidence that this assumption accurately describes the experiments in the present study and provide an explanation why Almeida et al. (2013) underestimated the formation rates.

It should be noted that the displayed experimental $J_{1.7nm}$ values (open red triangles in Fig. 1) are identical to the values from Almeida et al. (2013), while the sulfuric acid concentration has been corrected. In Almeida et al. (2013) data were shown from CLOUD4 (spring 2011) and CLOUD7 (fall 2012). For consistency, the sulfuric acid concentrations from the chemical ionization mass spectrometer (Kürten et al., 2011) were used, as the CI-APi-TOF was not available during CLOUD4. Especially during CLOUD7, the chemical ionization mass spectrometer (CIMS) showed relatively high sulfuric acid concentrations even when no sulfuric acid was produced from the UV light system inside the CLOUD chamber; no correction was applied for this effect in Almeida et al. (2013). However, taking into account a background subtraction leads to a shallower slope for $J_{1.7nm}$ vs. sulfuric acid and brings the corrected CIMS values in a good agreement with the sulfuric acid measured by the CI-APi-TOF. In the present study, the data from the CI-APi-TOF were used. The slope for $J_{1.7nm}$ vs. sulfuric acid now yields a value of close to 2, while the previously reported value was ~3.7 (Almeida et al., 2013). The higher value resulted from the bias in the sulfuric acid concentration and the consideration of data points at low sulfuric acid concentration, where new particle formation is significantly affected by losses to the chamber walls, which tends to bias the slope towards higher values (Ehrhart and Curtius, 2013).

3.2 Comparison between NPF rates from the kinetic model and SMPS measurements

The formation rates in Almeida et al. (2013) were calculated from measured particle number densities with a condensation particle counter that has a lower cut-off diameter of ~3 nm. The derivation of particle formation rates at 1.7 nm therefore required an extrapolation to the smaller diameter. With the available model, we are now, in principle, able to calculate NPF rates for any particle dimeter and compare the result to directly measured rates. This was done for the SMPS size channel corresponding to a mobility diameter of 4.3 nm ($J_{4.3nm}$) with the method described in section 2.2. Using the SMPS data has the advantage that the size-dependent loss rates can be accurately taken into account, which is not possible when only the total (non size-resolved) concentration from a condensation particle counter is available. On the other hand, the smallest SMPS size channels need to be corrected by large factors to account for losses and charging probability, which introduces uncertainty.

The result for $J_{4.3nm}$ is shown in Figure 1 together with the modeled particle formation rates for the same diameter. The agreement between modeled and measured NPF rates is very good indicating that the collision-controlled model accurately describes 4.3 nm particle production rates for these experiments. This is further evidence that particles are formed at the collision-limit. However, it is also an indication that the Almeida et al. (2013) data underestimate the NPF rates, which is further discussed in the following section.

Atmos. Chem. Phys. Discuss., https://doi.org/10.5194/acp-2017-636
Manuscript under review for journal Atmos. Chem. Phys.
Discussion started: 8 August 2017

Atmospheric Chemistry and Physics Discussions

3.3 Reconstruction model results

Recently, a new method was introduced, which allows the extrapolation of NPF rates determined at a larger size (d_{p2}) to a smaller diameter (d_{p1}). The advantage of that method is that the effect of cluster-cluster collisions (self-coagulation) can be accurately taken into account (Kürten et al., 2015a). So far, the method has not been tested for measured particle size distributions. However, the effect of cluster-cluster collisions should be largest in the case of collision-controlled nucleation since it results in the highest possible cluster (particle) concentrations for a given production rate of nucleating molecules. Therefore, the current data set is ideal for testing the new method. It requires the measured growth rate as an input parameter (equation (4)); this growth rate was derived from fitting a linear curve to the mode diameter determined from the SMPS size distribution (Hirsikko et al., 2005). It was then used as a constant (i.e., it was assumed that it is independent of size) for the full reconstruction of the size distribution, in order to obtain a formation rate at 1.7 nm. The growth rate could only be accurately determined for experiments with relatively high sulfuric acid concentration (above ~5×10^6 cm^{-3}); therefore, the reconstruction method was only tested for these conditions (Figure 1). The comparison with the modeled formation rates at the same size (1.7 nm) shows that the reconstruction method yields quite accurate results, highlighting the importance of cluster-cluster collisions in this chemical system. This explains why the Almeida et al. (2013) data strongly underestimate the particle formation rates.

While the reconstruction method gives good results in the present study, it needs to be mentioned that the errors for this method can become quite large. Small inaccuracies in the growth rate, can be blown up to very large uncertainties due to the non-linear nature of the method. This can be seen for some of the data points with large error bars in the positive direction. The errors are calculated by repeating the reconstruction with growth rates $GR \pm \mathrm{d}GR$, where dGR is the error from the fitted growth rate. Therefore, the accuracy of the method strongly depends on good growth rate measurements, and relies on the assumption that the growth rate does not change as a function of size. This seems to be a reasonable approximation for collision-controlled nucleation under the present conditions, but it could be different in other chemical systems.

3.4 Size distribution comparison between model and SMPS

Further comparison between modeled and measured data was performed for one experimental run (CLOUD7 run 1036.01) in which the particles were grown to sizes beyond 20 nm. Therefore, the time-dependent cluster/particle concentrations were modeled for a monomer production rate of 2.9×10^5 cm^{-3} s^{-1}, which results in a steady-state monomer concentration of 1.05×10^7 cm^{-3} for the model; this is the same as the measured sulfuric acid concentration. The measured and modeled size distributions are shown in Fig. 2 (upper panel) at four different times, i.e., at 1h, 2h, 4h and 6h after the start of the experiment. Given that there is no free parameter used in the model, the agreement is very good. For the earliest time shown (1h) the modeled concentrations overestimate the measured concentrations by up to 30%, whereas for the later times (≥ 4h) the model underestimates the measured concentrations by up to 30%. It is unclear whether these small discrepancies are due to SMPS measurement uncertainties, or if

the model does not include or accurately describe all the relevant processes. If, for example, the SMPS would underestimate the concentrations of the smaller particles (< ca. 15 nm) and overestimate those of the larger particles, the observed difference between modeled and measured concentrations could also be explained.

The lower panel of Fig. 2 compares measured and modeled aerosol volume concentrations. In order to enable direct comparison, the modeled size distribution was integrated starting at 4.3 nm since the SMPS did not capture smaller particles. In the beginning of the experiment the modeled aerosol volume is somewhat larger than the measured one, but, towards the end of the experiment (ca. 4h after its start), the volumes agree quite well, possible because the overestimated modeled particle number density at small diameters is compensated by the underestimated particle concentration in the larger size range (see Fig. 2, upper panel). This trend leads eventually to a slight underestimation of the aerosol volume by the model.

If one assumes that the SMPS is not responsible for the slight disagreement, then the following conclusions can be drawn regarding the accuracy of the model. The particle growth rate is almost perfectly represented by the model given the good agreement between the positions of the local maxima in the size distribution and the intersections between the size distributions and the x-axis. This good agreement between measured and modeled size distributions has already been demonstrated in Lehtipalo et al. (2016) for a particle diameter of 2 nm. The results shown here indicate that no significant condensation of other trace gases contribute to the growth of particles because, in this case, the measured particle size distributions would be shifted towards larger diameters compared to the model.

The good agreement between model and measurement is also a confirmation of the effect of van der Waals forces, when a Hamaker constant of 6.4×10^{-20} J is used, a value that has been demonstrated previously to represent particle size distribution dynamics correctly (McMurry, 1980; Chan and Mozurkewich, 2001; Kürten et al., 2014; Lehtipalo et al., 2016). Regarding the underestimation of the modeled size distribution for diameters ≳15 nm, one explanation could be that the size-dependent particle loss rates in the CLOUD chamber are weaker than assumed ($k_w \sim D^{0.5}$; see equation (2)). A weaker size dependence would lead to higher predicted particle concentrations at larger sizes (Park et al., 2001). However, no evidence was found from the existing CLOUD data that this is the case. Dedicated wall loss experiments could be performed in the future to investigate this hypothesis further.

3.5 Comparison of CLOUD chamber data to flow tube measurements by Jen et al. (2016a)

The data presented in the previous sections provide evidence that the new particle formation in the sulfuric acid-dimethylamine system during CLOUD7 proceeds at rates that are consistent with collision-controlled nucleation, in agreement with results for this data set obtained using different approaches (Kürten et al., 2014; Lehtipalo et al., 2016). However, measured cluster concentrations for the sulfuric acid-dimethylamine system from flow tube experiments indicated that finite evaporation rates exist for some clusters (Jen et al., 2014; Jen et al., 2016a). This was supported by the observation that diamines can yield even higher formation rates than amines for some conditions (Jen et al., 2016b). In this section, we compare the results by Jen et al. (2016a) to the results from the present study. In order to perform the comparison, the model described in section 2.4 was expanded in a way that allows to calculate the concentrations of

Atmos. Chem. Phys. Discuss., https://doi.org/10.5194/acp-2017-636
Manuscript under review for journal Atmos. Chem. Phys.
Discussion started: 8 August 2017

Atmospheric Chemistry and Physics Discussions

the monomer, dimer and trimer as a function of their dimethylamine content. In the following A_xB_y denotes the concentration of a cluster containing x sulfuric acid (x = 1 for the monomer) and y base (dimethylamine) molecules. It is assumed that $x \geq y$ for all clusters, i.e., the number of bases is always smaller or equal to the number of acid molecules. When the total monomer concentration ($A_1 + A_1B_1$) is fixed then the following equations result, i.e. for the A_1B_1 cluster:

$$\frac{dA_1B_1}{dt} = K_{1,1} \cdot B_1 \cdot A_1 - \left(k_{1,w} + k_{dil} + k_{e,A_1B_1} + \sum_{j=1}^{Nmax} K_{1,j} \cdot N_j\right) \cdot A_1B_1, \quad (10)$$

for the two different identities of the sulfuric acid dimer:

$$\frac{dA_2B_1}{dt} = \left(K_{1,1} \cdot A_1 \cdot A_1B_1 + k_{e,A_3B_1} \cdot A_3B_1\right) - \left(k_{w,2} + k_{dil} + K_{1,2} \cdot B_1 + \sum_{j=1}^{N} K_{j,2} \cdot N_j\right) \cdot A_2B_1, \quad (11a)$$

$$\frac{dA_2B_2}{dt} = \left(0.5 \cdot K_{1,1} \cdot A_1B_1 \cdot A_1B_1 + K_{1,2} \cdot B_1 \cdot A_2B_1 + k_{e,A_3B_2} \cdot A_3B_2\right) - \left(k_{w,2} + k_{dil} + \sum_{j=1}^{N} K_{j,2} \cdot N_j\right) \cdot A_2B_2, \quad (11b)$$

and for the three different identities of the sulfuric acid trimer:

$$\frac{dA_3B_1}{dt} = \left(K_{1,2} \cdot A_1 \cdot A_2B_1\right) - \left(k_{w,3} + k_{dil} + k_{e,A_3B_1} + K_{1,3} \cdot B_1 + \sum_{j=1}^{N} K_{j,3} \cdot N_j\right) \cdot A_3B_1, \quad (12a)$$

$$\frac{dA_3B_2}{dt} = \left(K_{1,2} \cdot A_1B_1 \cdot A_2B_1 + K_{1,2} \cdot A_1 \cdot A_2B_2 + K_{1,3} \cdot B_1 \cdot A_3B_1\right) - \left(k_{w,3} + k_{dil} + k_{e,A_3B_2} + K_{1,3} \cdot B_1 + \sum_{j=1}^{N} K_{j,3} \cdot N_j\right) \cdot A_3B_2, \quad (12b)$$

$$\frac{dA_3B_3}{dt} = \left(K_{1,2} \cdot A_1B_1 \cdot A_2B_2 + K_{1,3} \cdot B_1 \cdot A_3B_2\right) - \left(k_{w,3} + k_{dil} + \sum_{j=1}^{N} K_{j,3} \cdot N_j\right) \cdot A_3B_3. \quad (12c)$$

Stable tetramers are formed from trimers and dimers; in order to be stable they need to contain at least two base molecules (Jen et al., 2016a):

$$\frac{dN_4}{dt} = \left(K_{1,3} \cdot A_1B_1 \cdot A_3B_1 + K_{1,3} \cdot N_1 \cdot (A_3B_2 + A_3B_3) + 0.5 \cdot K_{2,2} \cdot N_2 \cdot N_2\right) - \left(k_{w,4} + k_{dil} + \sum_{j=1}^{N} K_{j,4} \cdot N_j\right) \cdot N_4. \quad (13)$$

The concentrations of larger clusters and particles are calculated with the same method as described in section 2.4. The evaporation rates considered are $k_{e,A1B1}$ = 0.1 s^{-1}, $k_{e,A1B1}$ = 1 s^{-1} and $k_{e,A1B1}$ = 1 s^{-1} (Jen et al., 2016a). Pure acid clusters are assumed to evaporate much more rapidly at this temperature (278 K) and are, therefore, not considered (Hanson and Lovejoy, 2006). The cluster concentrations reported in the following refer to the number of acid molecules in the cluster, i.e., $N_1 = A_1 + A_1B_1$, $N_2 = A_2B_1 + A_2B_2$ and $N_3 = A_3B_1 + A_3B_2 + A_3B_3$.

Figure 3 shows a comparison between calculated cluster (dimer, trimer, tetramer and pentamer) concentrations using collision-controlled nucleation (section 2.4) and the model described in this section. When a DMA mixing ratio of 40 pptv is used (this was the average mixing ratio of DMA during the CLOUD7 experiments), there is almost no difference between

the two scenarios. This indicates that, under the CLOUD7 conditions, new particle formation proceeded at almost the same rates that result for collision-controlled nucleation. Nevertheless, this does not imply that all cluster evaporation rates are zero. The conditions are only such that, due to the high DMA mixing ratio, most of the clusters (including the monomer) contain as many DMA molecules as sulfuric acid molecules; if the ratio between acid and base is 1:1 the clusters are most stable if their evaporation rates are assumed zero as in the model by Jen et al. (2016a). This assumption is supported by quantum chemical calculations (Ortega et al., 2012).

The effect of the dimethylamine concentration on the cluster concentrations and on the particle formation rate was further investigated. The lower panel of Fig. 3 shows that the cluster concentrations and the NPF rate at 1.7 nm decrease with decreasing DMA levels. The figure shows the concentrations and the NPF rate normalized by the results for the collision-limit. The NPF rate drops by about a factor of three when DMA is reduced to 2.5×10^{7} cm^{-3} (~ 1 pptv). Below that level, the reduction in *J* and in the trimer, tetramer, and pentamer concentrations is approximately linear with DMA. The dimer is less affected since, in the model, its evaporation rates are set to zero while the evaporating trimers contribute to the dimer concentration. From this perspective, very high particle formation rates should be observed even at DMA mixing ratios around 1 pptv, which should be almost indistinguishable from rates calculated for collision-controlled nucleation. Possibilities why such high rates have so far not been observed are discussed in section 4.

3.6 Simulation of atmospheric nucleation at low DMA mixing ratio

A comparison between modeled and measured atmospheric data is shown in Fig. 4. The measured data at a mobility diameter of 1.5 nm are from a station in a boreal forest in Finland (Kulmala et al., 2013). Sipilä et al. (2015) reported recently that no dimethylamine could be detected at this site. However, the detection limit of the instrument was ~0.12 pptv; this would leave open the possibility that tiny concentrations of DMA could be present. Therefore, the model described above was used to estimate what NPF rates would result for a comparable low dimethylamine mixing ratio of 0.1 pptv for varying concentrations of sulfuric acid. The adjusted model described in section 3.5 was used to calculate the NPF rates at 1.5 nm (cluster containing six sulfuric acid and six DMA molecules) in order to be consistent with the atmospheric measurements (Kulmala et al., 2013). The effect of the condensation sink by pre-existing particles that can scavenge sulfuric acid and the newly-formed particles was considered by introducing a monomodal log-normal size distribution with a mode diameter of 100 nm and a geometric standard deviation of 1.5. The total particle concentration of the pre-existing aerosol was scaled such that the condensation sink is 2×10^{-3} s^{-1} for sulfuric acid. To cover a wide size range the geometric factor for the size bin was increased from 1.015 to 1.035. For these simulations, the wall loss factor and the dilution rate constant were set to zero.

The results from Fig. 4 (green line) indicate that the expected NPF rates would be higher than the measured rates in most cases; especially at high sulfuric acid concentrations, the calculated rates are significantly faster. This is due to a steeper slope of the NPF rates as a function of sulfuric acid. However, keeping the dimethylamine mixing ratio constant at 0.1 pptv for all acid concentrations is probably not realistic for two reasons: (1) a high sulfuric acid concentration is, in some cases, related to a high OH concentration; OH can, however, deplete

DMA in the gas phase; and (2) the DMA is consumed by the newly-formed particles. In order to consider these effects, the DMA concentration is assumed to scale inversely with the sulfuric acid concentration, i.e., at 1×10^6 cm^{-3} of sulfuric acid, the DMA mixing ratio is 0.1 pptv, while it is only 0.01 pptv at 1×10^7 cm^{-3} of sulfuric acid. This is a very strong assumption about the connection between sulfuric acid and DMA, but the scenario (magenta curve) results in much slower NPF rates at high acid concentrations and the model curve can in principle replicate the measured NPF rates including the shallower slope. It has to be noted that very small DMA mixing ratios (e.g., 0.01 pptv equal ~2.5×10^5 cm^{-3}) are assumed, which are up to ~100 times lower than the acid concentration. Therefore, the scenario might seem unphysical at the first glance. However, not all amine molecules are bound to sulfuric acid. The model indicates that only a tiny fraction of the sulfuric acid monomer contains a dimethylamine molecule, so there would still be a high fraction of free DMA. What is, however, required for such a scenario is a local source term that replenishes the DMA; otherwise the DMA would be rapidly depleted by the condensation sink. Evidence that amine mixing ratios decreased during new particle formation events has been reported (Kürten et al., 2016b).

In addition, it should be noted that we do not attempt to explain new particle formation in the boreal forest from sulfuric acid and dimethylamine as no direct evidence has been found that this occurs. Rather, our analysis shows that amine mixing ratios below current detection limits could lead to significant NPF rates.

4. DISCUSSION

This study confirms the previous conclusion that new particle formation in the sulfuric acid-dimethylamine-water system can proceed at or close to the collision-controlled limit (Kürten et al., 2014; Lehtipalo et al., 2016). This is the case for sulfuric acid concentrations between 1×10^6 and 3×10^7 cm^{-3} and dimethylamine mixing ratios around 40 pptv at 278 K and 38% RH. For these conditions particle formation rates and size distributions can be reproduced with high accuracy by an aerosol model that assumes that particle growth is exclusively due the irreversible addition of H_2SO_4•$(CH_3)_2NH$ "monomers" and coagulation. Even when evaporation rates for the less stable clusters are introduced in the model (Jen et al., 2016a) the resulting particle formation rates are effectively indistinguishable from the kinetic model results for CLOUD7 conditions. This indicates that the flow tube study by Jen et al. (2016a) and the CLOUD data are in good agreement. The fact that the measured particle size distribution can be reproduced with good accuracy shows that neither water nor other species contribute significantly to particle growth during these CLOUD chamber experiments. Water could play a role at higher relative humidities, however, in addition, it is not clear yet how temperature influences the cluster evaporation rates. The evaporation rates from Jen et al. (2016a) were derived at temperatures close to 300 K; therefore the simulation of nucleation in the CLOUD chamber (278 K) using the Jen et al. (2016a) rate parameters is likely to overestimate the effect of cluster evaporation.

The question of why sulfuric acid-amine nucleation is rarely observed in the atmosphere is still open. Jen et al. (2016a) reported that clusters that contain equal numbers of dimethylamine and sulfuric acid molecules are ionized at reduced efficiencies than more acidic clusters with

the commonly used $NO_3^-(HNO_3)_{0-2}$ reagent ions. Still, Kürten et al. (2014) observed high concentrations for large clusters containing acid and base at an average ratio of 1:1. A reduced detection efficiency was also reported but the reduced sensitivity (in relation to the monomer) was, e.g. only a factor of 3 for the trimer containing DMA. Using the model results from section 3.5 the expected trimer concentration at 5×10^6 cm^{-3} of sulfuric acid and 1 pptv of DMA should be ~1×10^5 cm^{-3}. Even when the detection efficiency for the trimer was reduced by a factor of 3, such a concentration should still be well above the detection limit of a CI-APi-TOF. However, no sulfuric acid trimers could be detected in a field study where amines were present at levels above 1 pptv (Kürten et al., 2016b). It is, therefore, possible that any amines present were not suitable for nucleation. Therefore, application of methods capable of amine speciation should be applied more widely in atmospheric measurements (Place et al., 2017).

Several CLOUD papers reported particle formation rates for a diameter of 1.7 nm. Some of these published formation rates were derived from direct measurements using particle counters with cut-off diameters close to 1.7 nm (Riccobono et al., 2014; Duplissy et al., 2016), while other reported NPF rates were derived from process models describing the nucleation process in the CLOUD chamber (Kirkby et al., 2011; Kirkby et al., 2016). Therefore, no extrapolation of the NPF rates from a larger threshold diameter was performed, which could have led to an underestimation due to missing self-coagulation. Besides Almeida et al. (2013), the data set reported by Dunne et al. (2016) and Kürten et al. (2016a) did make use of the NPF rate extrapolation method from 3.2 to 1.7 nm without taking into account the effect of self-coagulation. However, the reported formation rates are, in almost all cases, considerably slower than those for the collision-controlled limit at a given sulfuric acid concentration since no dimethylamine was present in the CLOUD chamber (Dunne et al., 2016; Kürten et al., 2016a). The chemical system in these studies was the binary system, (H_2SO_4 and H_2O) and the ternary system involving ammonia. The conditions only approached the collision-controlled limit at the lowest temperature (210 K) when the highest ammonia mixing ratio of ~6 pptv was investigated (Kürten et al., 2015b). However, even under these conditions, the reported rates are only about a factor of 2 slower than the collision-controlled limit (Kürten et al., 2016a). This is probably related to the low acid concentrations ($\leq 3\times10^6$ cm^{-3}) in these experiments, where the self-coagulation effect is not as strong as at higher acid concentration (see Fig. 1) when wall loss and dilution lead to decreased cluster concentrations relative to the monomer. This indicates that previously published CLOUD results, other than the Almeida et al. (2013) data, are most likely not significantly affected.

McMurry and Li (2017) have recently investigated the effect of the wall loss and dilution rate on new particle formation with their numeric model, which uses dimensionless parameters. In order to allow for a comparison between McMurry and Li (2017) and the present study, information on the parameters *W* (describing wall loss) and *M* (describing dilution) is provided (see McMurry and Li, 2017, for the exact definitions). These parameters range from 0.04 to 0.7 (*W*) and 2×10^{-3} to 4×10^{-2} (*M*) for the experiments shown in this study. The monomer production rate (P_1) ranges from 7×10^3 to 2×10^6 cm^{-3} s^{-1}.

Atmos. Chem. Phys. Discuss., https://doi.org/10.5194/acp-2017-636
Manuscript under review for journal Atmos. Chem. Phys.
Discussion started: 8 August 2017

Atmospheric Chemistry and Physics Discussions

5. SUMMARY AND CONCLUSIONS

New particle formation rates from CLOUD chamber measurements for the sulfuric acid-dimethylamine-water system were re-analyzed. It was found that the previously published rates by Almeida et al. (2013) underestimate the NPF rates by up to a factor of ~50 at high acid concentrations (~1×10^7 cm^{-3}). The reason for this underestimation is the effect of self-coagulation that contributes efficiently to the loss of small particles in the size range relevant for the data analysis (between 1.7 and 3.2 nm). The previously used method for extrapolating the NPF rates from 3.2 nm to 1.7 nm did not include this effect and therefore the correction factors were too small. Using an advanced reconstruction method that accounts for the effect of self-coagulation yields much higher NPF rates (Kürten et al., 2015a). These corrected NPF rates are in good agreement with rates calculated from an aerosol model assuming collision-controlled nucleation and with measured NPF rates from SMPS data. Furthermore, the model can reproduce the measured size distribution with good accuracy up to ~30 nm.

Extending the aerosol model by including evaporation rates for some clusters (see Jen et al., 2016a) still yields good agreement between modeled and measured CLOUD NPF rates and cluster concentrations. This indicates that the data from the flow tube study by Jen et al. (2016a) and from CLOUD (Kürten et al., 2014) are consistent.

The aerosol model including the evaporation rates is also used to simulate atmospheric new particle formation. Assuming low DMA mixing ratios ($\leq$ 0.1 pptv) the atmospheric NPF rates can be reproduced reasonably well; however, the relatively low slope of NPF rate vs. sulfuric acid concentration requires the use of a decreasing DMA concentration with increasing sulfuric acid concentration. Such conditions are, however, reasonable because the incorporation of amines into newly formed particles leads to depletion of the amines, while H_2SO_4 is efficiently replenished by the production from OH and SO_2.

The above findings raise some further conclusions and questions. These are in part related to the rare detection of sulfuric acid-amine nucleation in the atmosphere. Only one study has so far reported sulfuric acid-amine nucleation (Zhao et al., 2011). The nucleation of sulfuric acid-amines could occur, however, more often than currently thought.

– It is unclear to what extent previously published atmospheric NPF rates are affected by incomplete *J* extrapolations. Some *J* measurements were made at diameters close to 3 nm and extrapolated to a smaller size. If self-coagulation were important, the formation rates at the small sizes could be significantly underestimated, and, therefore, in reality be much closer to rates consistent with collision-controlled nucleation than previously thought. In such a case, DMA (or other equally effective amines) could have been responsible for nucleation as they are among the most potent nucleation precursors (in combination with sulfuric acid). To avoid such ambiguities, the NPF rates should, in the future, be directly measured at small diameters whenever possible.

– Better gas-phase amine (base) measurements are needed. Detection limits need to reach mixing ratios even below 0.1 pptv; ideally the methods should also be capable of speciating the amines (discriminate e.g. dimethylamine from ethylamine, which have the same mass

when measured by mass spectrometry but probably behave differently in terms of their contribution to NPF).

– It is not clear why no clusters containing three or more sulfuric acid molecules are frequently observed during atmospheric new particle formation when amines are expected to be present. This could be due to incorrect assumptions about the amine concentrations, the amine identities, or a reduced detection efficiency of chemical ionization mass spectrometers (Jen et al., 2016a). The potential formation of complex multi-species clusters (containing sulfuric acid, amines, ammonia and oxidized organics) in the atmosphere could distribute the clusters over many different identities and therefore result in concentrations too low to be detected by the current instrumentation for the individual species.

The overall contribution of amines to atmospheric nucleation can only be quantified after these issues are understood. Besides further atmospheric measurements, controlled laboratory measurements are necessary. Of special interest are the temperature dependent evaporation rates of the relevant sulfuric-acid amine clusters.

DATA AVAILABILITY

Data used in this study can be obtained by sending an email to the corresponding author.

ACKNOWLEDGEMENTS

Funding from the German Federal Ministry of Education and Research (grant no. 01LK1222A) and the Marie Curie Initial Training Network "CLOUD-TRAIN" (grant no. 316662) is gratefully acknowledged. PHM's and CL's contributions to this work were supported by the US Department of Energy's Atmospheric System Research program, an Office of Science, Office of Biological and Environmental Research, under grant number DE-SC0011780. RCF acknowledges funding from the NSF Grants 1439551 and 1602086. MRP appreciates funding from the Academy of Finland (project no. 299574). KL thanks the European Union's Horizon 2020 research and innovation programme under the Marie Sklodowska-Curie grant agreement no. 656994 (nano-CAVa).

References

Almeida, J., Schobesberger, S., Kürten, A., Ortega, I. K., Kupiainen-Määttä, O., Praplan, A. P., Adamov, A., Amorim, A., Bianchi, F., Breitenlechner, M., David, A., Dommen, J., Donahue, N. M., Downard, A., Dunne, E. M., Duplissy, J., Ehrhart, S., Flagan, R. C., Franchin, A., Guida, R., Hakala, J., Hansel, A., Heinritzi, M., Henschel, H., Jokinen, T., Junninen, H., Kajos, M., Kangasluoma, J., Keskinen, H., Kupc, A., Kurtén, T., Kvashin, A. N., Laaksonen, A., Lehtipalo, K., Leiminger, M., Leppä, J., Loukonen, V., Makhmutov, V., Mathot, S., McGrath, M. J., Nieminen, T., Olenius, T., Onnela, A., Petäjä, T., Riccobono, F., Riipinen, I., Rissanen, M., Rondo, L., Ruuskanen, T., Santos, F. D., Sarnela, N., Schallhart, S., Schnitzhofer, R., Seinfeld, J. H., Simon, M., Sipilä, M., Stozhkov, Y., Stratmann, F., Tomé, A., Tröstl, J., Tsagkogeorgas, G., Vaattovaara, P., Viisanen, Y., Virtanen, A., Vrtala, A., Wagner, P. E., Weingartner, E., Wex, H., Williamson, C., Wimmer, D., Ye, P., Yli-Juuti, T., Carslaw, K. S., Kulmala, M., Curtius, J., Baltensperger, U., Worsnop, D. R., Vehkamäki, H., and Kirkby, J.: Molecular understanding of sulphuric acid-amine particle nucleation in the atmosphere, *Nature*, 502, 359–363, doi: 10.1038/nature12663, 2013.

Ball, S. M., Hanson, D. R., Eisele, F. L., and McMurry, P. H.: Laboratory studies of particle nucleation: Initial results for H_2SO_4, H_2O, and NH_3 vapors, *J. Geophys. Res.-Atmos.*, 104, D19, 23709–23718, doi: 10.1029/1999JD900411, 1999.

Bergman, T., Laaksonen, A., Korhonen, H., Malila, J., Dunne, E. M., Mielonen, T., Lehtinen, K. E. J., Kühn, T., Arola, A., and Kokkola, H.: Geographical and diurnal features of amine-enhanced boundary layer nucleation, *J. Geophys. Res.-Atmos.*, 120, 9606–9624, doi: 10.1002/2015JD023181, 2015.

Berndt, T., Sipilä, M., Stratmann, F., Petäjä, T., Vanhanen, J., Mikkilä, J., Patokoski, J., Taipale, R., Mauldin III, R. L., and Kulmala, M.: Enhancement of atmospheric H_2SO_4 / H_2O nucleation: organic oxidation products versus amines, *Atmos. Chem. Phys.*, 14, 751–764, doi: 10.5194/acp-14-751-2014, 2014.

Bianchi, F., Praplan, A. P., Sarnela, N., Dommen, J., Kürten, A., Ortega, I. K., Schobesberger, S., Junninen, H., Simon, M., Tröstl, J., Jokinen, T., Sipilä, M., Adamov, A., Amorim, A., Almeida, J., Breitenlechner, M., Duplissy, J., Ehrhart, S., Flagan, R. C., Franchin, A., Hakala, J., Hansel, A., Heinritzi, M., Kangasluoma, J., Keskinen, H., Kim, J., Kirkby, J., Laaksonen, A., Lawler, M. J., Lehtipalo, K., Leiminger, M., Makhmutov, V., Mathot, S., Onnela, A., Petäjä, T., Riccobono, F., Rissanen, M. P., Rondo, L., Tomé, A., Virtanen, A., Viisanen, Y., Williamson, C., Wimmer, D., Winkler, P. M., Ye, P., Curtius, J., Kulmala, M., Worsnop, D. R., Donahue, N. M., and Baltensperger, U.: Insight into acid-base nucleation experiments by comparison of the chemical composition of positive, negative, and neutral clusters, *Environ. Sci. Technol.*, 48, 13675–13684, doi: 10.1021/es502380b, 2014.

731 Chan, T. W., and Mozurkewich, M.: Measurement of the coagulation rate constant for sulfuric
732 acid particles as a function of particle size using tandem differential mobility analysis, *J.*
733 *Aerosol Sci.*, 32, 321–339, doi: 10.1016/S0021-8502(00)00081-1, 2001.
734
735 Chen, M., Titcombe, M., Jiang, J., Jen, C., Kuang, C., Fischer, M. L., Eisele, F. L., Siepmann,
736 J. I., Hanson, D. R., Zhao, J., and McMurry, P. H.: Acid–base chemical reaction model for
737 nucleation rates in the polluted atmospheric boundary layer, *P. Natl. Acad. Sci. USA*, 109,
738 18713–18718, doi: 10.1073/pnas.1210285109, 2012.
739
740 Clark, W. E., and Whitby, K. T.: Measurements of aerosols produced by the photochemical
741 oxidation of SO_2 in air, *J. Colloid Interface Sci.*, 51, 477–490, doi: 10.1016/0021-
742 9797(75)90144-7, 1975.
743
744 Crounse, J. D., Nielsen, L. B., Jørgensen, S., Kjaergaard, H. G., and Wennberg, P. O.:
745 Autooxidation of organic compounds in the atmosphere, *J. Phys. Chem. Lett.*, 4, 3513–3520,
746 doi: 10.1021/jz4019207, 2013.
747
748 Crump, J. G., and Seinfeld, J. H.: Turbulent deposition and gravitational sedimentation of an
749 aerosol in a vessel of arbitrary shape, *J. Aerosol Sci.*, 12, 405–415, doi: 10.1016/0021-
750 8502(81)90036-7, 1981.
751
752 Dunne, E. M., Gordon, H., Kürten, A., Almeida, J., Duplissy, J., Williamson, C., Ortega, I. K.,
753 Pringle, K. J., Adamov, A., Baltensperger, U., Barmet, P., Benduhn, F., Bianchi, F.,
754 Breitenlechner, M., Clarke, A., Curtius, J., Dommen, J., Donahue, N. M., Ehrhart, S., Flagan,
755 R. C., Franchin, A., Guida, R., Hakala, J., Hansel, A., Heinritzi, M., Jokinen, T., Kangasluoma,
756 J., Kirkby, J., Kulmala, M., Kupc, A., Lawler, M. J., Lehtipalo, K., Makhmutov, V., Mann, G.,
757 Mathot, S., Merikanto, J., Miettinen, P., Nenes, A., Onnela, A., Rap, A., Reddington, C. L. S.,
758 Riccobono, F., Richards, N. A. D., Rissanen, M. P., Rondo, L., Sarnela, N., Schobesberger, S.,
759 Sengupta, K., Simon, M., Sipilä, M., Smith, J. N., Stozkhov, Y., Tomé, A., Tröstl, J., Wagner,
760 P. E., Wimmer, D., Winkler, P. M., Worsnop, D. R., and Carslaw, K. S.: Global atmospheric
761 particle formation from CERN CLOUD measurements, *Science*, 354, 1119–1124, doi:
762 10.1126/science.aaf2649, 2016.
763
764 Duplissy, J., Merikanto, J., Franchin, A., Tsagkogeorgas, G., Kangasluoma, J., Wimmer, D.,
765 Vuollekoski, H., Schobesberger, S., Lehtipalo, K., Flagan, R. C., Brus, D., Donahue, N. M.,
766 Vehkämäki, H., Almeida, J., Amorim, A., Barmet, P., Bianchi, F., Breitenlechner, M., Dunne,
767 E. M., Guida, R., Henschel, H., Junninen, H., Kirkby, J., Kürten, A., Kupc, A., Määttänen, A.,
768 Makhmutov, V., Mathot, S. , Nieminen, T., Onnela, A., Praplan, A. P., Riccobono, F., Rondo,
769 L., Steiner, G., Tome, A., Walther, H., Baltensperger, U., Carslaw, K. S., Dommen, J., Hansel,
770 A., Petäjä, T., Sipilä, M., Stratmann, F., Vrtala, A., Wagner, P. E., Worsnop, D. R., Curtius, J.,
771 and Kulmala, M.: Effect of ions on sulfuric acid-water binary particle formation II:
772 Experimental data and comparison with QC-normalized classical nucleation theory, *J.*
773 *Geophys. Res.-Atmos.*, 121, 1752–1775, doi: 10.1002/2015JD023539, 2016.
774

Ehrhart, S. and Curtius, J.: Influence of aerosol lifetime on the interpretation of nucleation experiments with respect to the first nucleation theorem, *Atmos. Chem. Phys.*, 13, 11465–11471, doi: 10.5194/acp-13-11465-2013, 2013.

Ehrhart, S., Ickes, L., Almeida, J., Amorim, A., Barmet, P., Bianchi, F., Dommen, J., Dunne, E. M., Duplissy, J., Franchin, A., Kangasluoma, J., Kirkby, J., Kürten, A., Kupc, A., Lehtipalo, K., Nieminen, T., Riccobono, F., Rondo, L., Schobesberger, S., Steiner, G., Tomé, A., Wimmer, D., Baltensperger, U., Wagner, P. E., and Curtius, J.: Comparison of the SAWNUC model with CLOUD measurements of sulphuric acid-water nucleation, *J. Geophys. Res.-Atmos.*, 121, 12401–12414, doi: 10.1002/2015JD023723, 2016.

Ehn, M., Thornton, J. A., Kleist, E., Sipilä, M., Junninen, H., Pullinen, I., Springer, M., Rubach, F., Tillmann, R., Lee, B., Lopez-Hilfiker, F., Andres, S., Acir, I.-H., Rissanen, M., Jokinen, T., Schobesberger, S., Kangasluoma, J., Kontkanen, J., Nieminen, T., Kurtén, T., Nielsen, L. B., Jørgensen, S., Kjaergaard, H. G., Canagaratna, M., Dal Maso, M., Berndt, T., Petäjä, T., Wahner, A., Kerminen, V.-M., Kulmala, M., Worsnop, D. R., Wildt, J., and Mentel, T. F.: A large source of low-volatility secondary organic aerosol, *Nature*, 506, 476–479, doi: 10.1038/nature13032, 2014.

Fiedler, V., Dal Maso, M., Boy, M., Aufmhoff, H., Hoffmann, J., Schuck, T., Birmili, W., Hanke, M., Uecker, J., Arnold, F., and Kulmala, M.: The contribution of sulphuric acid to atmospheric particle formation and growth: a comparison between boundary layers in Northern and Central Europe, *Atmos. Chem. Phys.*, 5, 1773–1785, doi: 10.5194/acp-5-1773-2005, 2005.

Freshour, N. A., Carlson, K. K., Melka, Y. A., Hinz, S., Panta, B., and Hanson, D. R.: Amine permeation sources characterized with acid neutralization and sensitivities of an amine mass spectrometer, *Atmos. Meas. Tech.*, 7, 3611–3621, doi: 10.5194/amt-7-3611-2014, 2014.

Glasoe, W. A., Volz, K., Panta, B., Freshour, N., Bachman, R., Hanson, D. R., McMurry, P. H., and Jen, C.: Sulfuric acid nucleation: An experimental study of the effect of seven bases, *J. Geophys. Res.-Atmos.*, 120, 1933–1950, doi: 10.1002/2014JD022730, 2015.

Gordon, H., Sengupta, K., Rap, A., Duplissy, J., Frege, C., Williamson, C., Heinritzi, M., Simon, M., Yan, C., Almeida, J., Tröstl, J., Nieminen, T., Ortega, I. K., Wagner, R., Dunne, E. M., Adamov, A., Amorim, A., Bernhammer, A. K., Bianchi, F., Breitenlechner, M., Brilke, S., Chen, X., Craven, J. S., Dias, A., Ehrhart, S., Fischer, L., Flagan, R. C., Franchin, A., Fuchs, C., Guida, R., Hakala, J., Hoyle, C. R., Jokinen, T., Junninen, H., Kangasluoma, J., Kim, J., Kirkby, J., Krapf, M., Kürten, A., Laaksonen, A., Lehtipalo, K., Makhmutov, V., Mathot, S., Molteni, U., Monks, S. A., Onnela, A., Peräkylä, O., Piel, F., Petäjä, T., Praplan, A. P., Pringle, K. J., Richards, N. A. D., Rissanen, M. P., Rondo, L., Sarnela, N., Schobesberger, S., Scott, C. E., Seinfeld, J. H., Sharma, S., Sipilä, M., Steiner, G., Stozhkov, Y., Stratmann, F., Tomé, A., Virtanen, A., Vogel, A. L., Wagner, A. C., Wagner, P. E., Weingartner, E., Wimmer, D., Winkler, P. M., Ye, P., Zhang, X., Hansel, A., Dommen, J., Donahue, N. M., Worsnop, D. R., Baltensperger, U., Kulmala, M., Curtius, J., and Carslaw, K. S.: Reduced anthropogenic aerosol

819 radiative forcing caused by biogenic new particle formation, *Proc. Natl. Acad. Sci. USA*, 113,
820 12053–12058, doi: 10.1073/pnas.1602360113, 2016.
821
822 Hamaker, H. C.: The London–van der Waals attraction between spherical particles, *Physica*, 4,
823 1058–1072, doi: 10.1016/S0031-8914(37)80203-7, 1937.
824
825 Hanson, D. R., and Eisele, F.: Diffusion of H_2SO_4 in humidified nitrogen: Hydrated H_2SO_4, *J.*
826 *Phys. Chem. A*, 104, 1715–1719, doi: 10.1021/jp993622j, 2000.
827
828 Hanson, D. R., and Lovejoy, E. R.: Measurement of the thermodynamics of the hydrated dimer
829 and trimer of sulfuric acid, *J. Phys. Chem. A*, 110, 9525–9528, doi: 10.1021/jp062844w, 2006.
830
831 Hinds, W. C.: Aerosol technology: Properties, behavior, and measurement of airborne particles,
832 second edition, John Wiley & Sons, Inc., 150–153, 1999.
833
834 Hirsikko, A., Laakso, L., Hõrrak, U., Aalto, P. P., Kerminen, V.-M., and Kulmala, M.: Annual
835 and size dependent variation of growth rates and ion concentrations in boreal forest, *Boreal*
836 *Environ. Res.*, 10, 357–369, 2005.
837
838 Jen, C., McMurry, P. H., and Hanson, D. R.: Stabilization of sulfuric acid dimers by ammonia,
839 methylamine, dimethylamine, and trimethylamine, *J. Geophys. Res.-Atmos.*, 119, 7502–7514,
840 doi: 10.1002/2014JD021592, 2014.
841
842 Jen, C. N., Zhao, J., McMurry, P. H., and Hanson, D. R.: Chemical ionization of clusters formed
843 from sulfuric acid and dimethylamine or diamines, *Atmos. Chem. Phys.*, 16, 12513–12529, doi:
844 10.5194/acp-16-12513-2016, 2016a.
845
846 Jen, C. N., R. Bachman, J. Zhao, P. H. McMurry, and D. R. Hanson: Diamine-sulfuric acid
847 reactions are a potent source of new particle formation, *Geophys. Res. Lett.*, 43, 867–873, doi:
848 10.1002/2015GL066958, 2016b.
849
850 Jokinen, T., Sipilä, M., Junninen, H., Ehn, M., Lönn, G., Hakala, J., Petäjä, T., Mauldin III, R.
851 L., Kulmala, M., and Worsnop. D. R.: Atmospheric sulphuric acid and neutral cluster
852 measurements using CI-APi-TOF, *Atmos. Chem. Phys.*, 12, 4117–4125, doi: 10.5194/acp-12-
853 4117-2012, 2012.
854
855 Jokinen, T., Berndt, T., Makkonen, R., Kerminen, V.-M., Junninen, H., Paasonen, P.,
856 Stratmann, F., Herrmann, H., Guenther, A. B., Worsnop, D. R., Kulmala, M., Ehn, M., and
857 Sipilä, M.: Production of extremely low volatile organic compounds from biogenic emissions:
858 Measured yields and atmospheric implications, *P. Natl. Acad. Sci. USA*, 112, 7123–7128, doi:
859 10.1073/pnas.1423977112, 2015.
860
861 Kirkby, J., Curtius, J., Almeida, J., Dunne, E., Duplissy, J., Ehrhart, S., Franchin, A., Gagné,
862 S., Ickes, L., Kürten, A., Kupc, A., Metzger, A., Riccobono, F., Rondo, L., Schobesberger, S.,

Tsagkogeorgas, G., Wimmer, D., Amorim, A., Bianchi, F., Breitenlechner, M., David, A., Dommen, J., Downard, A., Ehn, M., Flagan, R.C., Haider, S., Hansel, A., Hauser, D., Jud, W., Junninen, H., Kreissl, F., Kvashin, A., Laaksonen, A., Lehtipalo, K., Lima, J., Lovejoy, E. R., Makhmutov, V., Mathot, S., Mikkilä, J., Minginette, P., Mogo, S., Nieminen, T., Onnela, A., Pereira, P., Petäjä, T., Schnitzhofer, R., Seinfeld, J. H., Sipilä, M., Stozhkov, Y., Stratmann, F., Tomé, A., Vanhanen, J., Viisanen, Y., Vrtala, A., Wagner, P. E., Walther, H., Weingartner, E., Wex, H., Winkler, P. M., Carslaw, K. S., Worsnop, D. R., Baltensperger, U., and Kulmala, M.: Role of sulphuric acid, ammonia and galactic cosmic rays in atmospheric aerosol nucleation, *Nature*, 476, 429–435, doi: 10.1038/nature10343, 2011.

Kirkby, J., Duplissy, J., Sengupta, K., Frege, C., Gordon, H., Williamson, C., Heinritzi, M., Simon, M., Yan, C., Almeida, J., Tröstl, J., Nieminen, T., Ortega, I. K., Wagner, R., Adamov, A., Amorim, A., Bernhammer, A.-K., Bianchi, F., Breitenlechner, M., Brilke, S., Chen, X., Craven, J., Dias, A., Ehrhart, S., Flagan, R. C., Franchin, A., Fuchs, C., Guida, R., Hakala, J., Hoyle, C. R., Jokinen, T., Junninen, H., Kangasluoma, J., Kim, J., Krapf, M., Kürten, A., Laaksonen, A., Lehtipalo, K., Makhmutov, V., Mathot, S., Molteni, U., Onnela, A., Peräkylä, O., Piel, F., Petäjä, T., Praplan, A. P., Pringle, K., Rap, A., Richards, N. A. D., Riipinen, I., Rissanen, M. P., Rondo, L., Sarnela, N., Schobesberger, S., Scott, C. E., Seinfeld, J. H., Sipilä, M., Steiner, G., Stozhkov, Y., Stratmann, F., Tomé, A., Virtanen, A., Vogel, A. L., Wagner, A., Wagner, P. E., Weingartner, E., Wimmer, D., Winkler, P. M., Ye, P., Zhang, X., Hansel, A., Dommen, J., Donahue, N. M., Worsnop, D. R., Baltensperger, U., Kulmala, M., Carslaw, K. S., and Curtius, J.: Ion-induced nucleation of pure biogenic particles, *Nature*, 533, 521–526, doi: 10.1038/nature17953, 2016.

Ku, B. K., and Fernandez de la Mora, J.: Relation between electrical mobility, mass, and size for nanodrops 1–6.5 nm in diameter in air, *Aerosol Sci. Technol.*, 43, 241–249, doi: 10.1080/02786820802590510, 2009.

Kuang, C., McMurry, P. H., McCormick, A. V., and Eisele, F. L.: Dependence of nucleation rates on sulfuric acid vapor concentration in diverse atmospheric locations, *J. Geophys. Res.-Atmos.*, 113, D10209, doi: 10.1029/2007JD009253, 2008.

Kulmala, M., Vehkamäki, H., Petäjä, T., Dal Maso, M., Lauri, A., Kerminen, V.-M., Birmili, W., and McMurry, V.-M.: Formation and growth rates of ultrafine atmospheric particles: a review of observations, *J. Aerosol Sci.*, 35, 143–176, doi: 10.1016/j.jaerosci.2003.10.003, 2004.

Kulmala, M., Kontkanen, J., Junninen, H., Lehtipalo, K., Manninen, H. E., Nieminen, T., Petäjä, T., Sipilä, M., Schobesberger, S., Rantala, P., Franchin, A., Jokinen, T., Järvinen, E., Äijälä, M., Kangasluoma, J., Hakala, J., Aalto, P. P., Paasonen, P., Mikkilä, J., Vanhanen, J., Aalto, J., Hakola, H., Makkonen, U., Ruuskanen, T., Mauldin III, R. L., Duplissy, J., Vehkamäki, H., Bäck, J., Kortelainen, A., Riipinen, I., Kurtén, T., Johnston, M. V., Smith, J. N., Ehn, M., Mentel, T. F., Lehtinen, K. E. J., Laaksonen, A., Kerminen, V.-M., and Worsnop, D. R.: Direct observations of atmospheric aerosol nucleation, *Science*, 339, 943–946, doi: 10.1126/science.1227385, 2013.

907
908 Kupc, A., Amorim, A., Curtius, J., Danielczok, A., Duplissy, J., Ehrhart, S., Walther, H., Ickes,
909 L., Kirkby, J., Kürten, A., Lima, J. M., Mathot, S., Minginette, P., Onnela, A., Rondo, L., and
910 Wagner, P. E.: A fibre-optic UV system for H_2SO_4 production in aerosol chambers causing
911 minimal thermal effects, *J. Aerosol Sci.*, 42, 532–543, doi: 10.1016/j.jaerosci.2011.05.001,
912 2011.
913
914 Kürten, A., Rondo, L., Ehrhart, S., and Curtius, J.: Performance of a corona ion source for
915 measurement of sulfuric acid by chemical ionization mass spectrometry, *Atmos. Meas. Tech.*,
916 4, 437–443, doi: 10.5194/amt-4-437-2011, 2011.
917
918 Kürten, A., Jokinen, T., Simon, M., Sipilä, M., Sarnela, N., Junninen, H., Adamov, A., Almeida,
919 J., Amorim, A., Bianchi, F., Breitenlechner, M., Dommen, J., Donahue, N. M., Duplissy, J.,
920 Ehrhart, S., Flagan, R. C., Franchin, A., Hakala, J., Hansel, A., Heinritzi, M., Hutterli, M.,
921 Kangasluoma, J., Kirkby, J., Laaksonen, A., Lehtipalo, K., Leiminger, M., Makhmutov, V.,
922 Mathot, S., Onnela, A., Petäjä, T., Praplan, A. P., Riccobono, F., Rissanen, M. P., Rondo, L.,
923 Schobesberger, S., Seinfeld, J. H., Steiner, G., Tomé, A., Tröstl, J., Winkler, P. M., Williamson,
924 C., Wimmer, D., Ye, P., Baltensperger, U., Carslaw, K. S., Kulmala, M., Worsnop, D. R., and
925 Curtius, J.: Neutral molecular cluster formation of sulfuric acid-dimethylamine observed in
926 real-time under atmospheric conditions, *P. Natl. Acad. Sci. USA*, 111, 15019–15024, doi:
927 10.1073/pnas.1404853111, 2014.
928
929 Kürten, A., Williamson, C., Almeida, J., Kirkby, J., and Curtius, J: On the derivation of particle
930 nucleation rates from experimental formation rates, *Atmos. Chem. Phys.*, 15, 4063–4075, doi:
931 10.5194/acp-15-4063-2015, 2015a.
932
933 Kürten, A., Münch, S., Rondo, L., Bianchi, F., Duplissy, J., Jokinen, T., Junninen, H., Sarnela,
934 N. Schobesberger, S., Simon, M., Sipilä, M. Almeida, J., Amorim, A., Dommen, J., Donahue,
935 N. M., Dunne, M., Flagan, R. C., Franchin, A., Kirkby, J., Kupc, A., Makhmutov, V., Petäjä,
936 T. Praplan, A. P., Riccobono, F., Steiner, G., Tomé, A., Tsagkogeorgas, G., Wagner, P. E.,
937 Wimmer, D., Baltensperger, U., Kulmala, M., Worsnop, D. R., and Curtius, J.:
938 Thermodynamics of the formation of sulfuric acid dimers in the binary (H_2SO_4-H_2O) and
939 ternary (H_2SO_4-H_2O-NH_3) system, *Atmos. Chem. Phys.*, 15, 10701–10721, doi: 10.5194/acp-
940 15-10701-2015, 2015b.
941
942 Kürten, A., Bianchi, F., Almeida, J., Kupiainen-Määttä, O., Dunne, E. M., Duplissy, J.,
943 Williamson, C., Barmet, P., Breitenlechner, M., Dommen, J., Donahue, N. M., Flagan, R. C.,
944 Franchin, A., Gordon, H., Hakala, J., Hansel, A., Heinritzi, M., Ickes, L., Jokinen, T.,
945 Kangasluoma, J., Kim, J., Kirkby, J., Kupc, A., Lehtipalo, K., Leiminger, M., Makhmutov, V.,
946 Onnela, A., Ortega, I. K., Petäjä, T., Praplan, A. P., Riccobono, F., Rissanen, M. P., Rondo, L.,
947 Schnitzhofer, R., Schobesberger, S., Smith, J. N., Steiner, G., Stozhkov, Y., Tomé, A., Tröstl,
948 J., Tsagkogeorgas, G., Wagner, P. E., Wimmer, D., Ye, P., Baltensperger, U., Carslaw, K.,
949 Kulmala, M., and Curtius, J.: Experimental particle formation rates spanning tropospheric

sulfuric acid and ammonia abundances, ion production rates and temperatures, *J. Geophys. Res.-Atmos.*, 121, 12377–12400, doi: 10.1002/2015JD023908, 2016a.

Kürten, A., Bergen, A., Heinritzi, M., Leiminger, M., Lorenz, V., Piel, F., Simon, M., Sitals, R., Wagner, A. C., and Curtius, J.: Observation of new particle formation and measurement of sulfuric acid, ammonia, amines and highly oxidized organic molecules at a rural site in central Germany, *Atmos. Chem. Phys.*, 16, 12793–12813, doi: 10.5194/acp-16-12793-2016, 2016b.

Kurtén, T., Loukonen, V., Vehkamäki, H., and Kulmala, M.: Amines are likely to enhance neutral and ion-induced sulfuric acid-water nucleation in the atmosphere more effectively than ammonia, *Atmos. Chem. Phys.*, 8, 4095–4103, doi: 10.5194/acp-8-4095-2008, 2008.

Lee, S.-H., Reeves, J. M., Wilson, J. C., Hunton, D. E., Viggiano, A. A., Miller, T. M., Ballenthin, J. O., and Lait, L. R.: Particle formation by ion nucleation in the upper troposphere and lower stratosphere, *Science*, 301, 1886–1889, doi: 10.1126/science.1087236, 2003.

Lehtipalo, K., Rondo, L., Kontkanen, J., Schobesberger, S., Jokinen, T., Sarnela, N., Kürten, A., Ehrhart, S., Franchin, A., Nieminen, T., Riccobono, F., Sipilä, M., Yli-Juuti, T., Duplissy, J., Adamov, A., Ahlm, L., Almeida, J., Amorim, A., Bianchi, F., Breitenlechner, M., Dommen, J., Downard, A. J., Dunne, E. M., Flagan, R. C., Guida, R., Hakala, J., Hansel, A., Jud, W., Kangasluoma, J., Kerminen, V.-M., Keskinen, H., Kim, J., Kirkby, J., Kupc, A., Kupiainen-Määttä, O., Laaksonen, A., Lawler, M. J., Leiminger, M., Mathot, S., Olenius, T., Ortega, I. K., Onnela, A., Petäjä, T., Praplan, A., Rissanen, M. P., Ruuskanen, T., Santos, F. D., Schallhart, S., Schnitzhofer, R., Simon, M., Smith, J. N., Tröstl, J., Tsagkogeorgas, G., Tomé, A., Vaattovaara, P., Vehkamäki, H., Vrtala, A. E., Wagner, P. E., Williamson, C., Wimmer, D., Winkler, P. M., Virtanen, A., Donahue, N. M., Carslaw, K. S., Baltensperger, U., Riipinen, I., Curtius, J., Worsnop, D. R., and Kulmala, M.: The effect of acid–base clustering and ions on the growth of atmospheric nano-particles, *Nature Commun.*, 7, 11594, doi: 10.1038/ncomms11594, 2016.

Lovejoy, E. R., Curtius, J., and Froyd, K. D.: Atmospheric ion-induced nucleation of sulfuric acid and water, *J. Geophys. Res.-Atmos.*, 109, D08204, doi: 10.1029/2003JD004460, 2004.

McMurry, P. H.: Photochemical Aerosol Formation from SO_2: A theoretical analysis of smog chamber data, *J. Colloid Interf. Sci.*, 78, 513–527, doi: 10.1016/0021-9797(80)90589-5, 1980.

McMurry, P. H., and Li, C.: The dynamic behavior of nucleating aerosols in constant reaction rate systems: Dimensional analysis and generic numerical solutions, *Aerosol Sci. Technol.*, accepted, 2017.

Nadykto, A. B., Yu, F., Jakovleva, M. V., Herb, J., and Xu, Y.: Amines in the Earth's atmosphere: A density functional theory study of the thermochemistry of pre-nucleation clusters, *Entropy*, 13, 554–569; doi: 10.3390/e13020554, 2011.

994 Ortega, I. K., Kupiainen, O., Kurtén, T., Olenius, T., Wilkman, O., McGrath, M. J., Loukonen,
995 V., and Vehkamäki, H.: From quantum chemical formation free energies to evaporation rates,
996 *Atmos. Chem. Phys.*, 12, 225–235, doi: 10.5194/acp-12-225-2012, 2012.
997
998 Park, S. H., Kim, H. O., Han, Y. T., Kwon, S. B., and Lee, K. W.: Wall loss rate of polydispersed
999 aerosols, *Aerosol Sci. Technol.*, 35, 710–717, doi: 10.1080/02786820152546752, 2001.
1000
1001 Place, B. K., Quilty, A. T., Di Lorenzo, R. A., Ziegler, S. E., and VandenBoer, T. C.:
1002 Quantitation of 11 alkylamines in atmospheric samples: separating structural isomers by ion
1003 chromatography, *Atmos. Meas. Tech.*, 10, 1061–1078, doi: 10.5194/amt-10-1061-2017, 2017.
1004
1005 Praplan, A. P., Bianchi, F., Dommen, J., and Baltensperger, U.: Dimethylamine and ammonia
1006 measurements with ion chromatography during the CLOUD4 campaign, *Atmos. Meas. Tech.*,
1007 5, 2161–2167, doi: 10.5194/amt-5-2161-2012, 2012.
1008
1009 Rao, N. P., and McMurry, P. H.: Nucleation and Growth of Aerosol in Chemically Reacting
1010 Systems: A Theoretical Study of the Near-Collision-Controlled Regime, *Aerosol Sci. Technol.*,
1011 11, 120–132, doi: 10.1080/02786828908959305, 1989.
1012
1013 Qiu, C., and Zhang, R.: Physiochemical properties of alkylaminium sulfates: hygroscopicity,
1014 thermostability, and density, *Environ. Sci. Technol.*, 46, 4474–4480, doi: 10.1021/es3004377,
1015 2012.
1016
1017 Riccobono, F., Schobesberger, S., Scott, C. E., Dommen, J., Ortega, I. K., Rondo, L., Almeida,
1018 J., Amorim, A., Bianchi, F., Breitenlechner, M., David, A., Downard, A., Dunne, E. M.,
1019 Duplissy, J., Ehrhart, S., Flagan, R. C., Franchin, A., Hansel, A., Junninen, H., Kajos, M.,
1020 Keskinen, H., Kupc, A., Kürten, A., Kvashin, A. N., Laaksonen, A., Lehtipalo, K., Makhmutov,
1021 V., Mathot, S., Nieminen, T., Onnela, A., Petäjä, T., Praplan, A. P., Santos, F. D., Schallhart,
1022 S., Seinfeld, J. H., Sipilä, M., Spracklen, D. V., Stozhkov, Y., Stratmann, F., Tomé, A.,
1023 Tsagkogeorgas, G., Vaattovaara, P., Viisanen, Y., Vrtala, A., Wagner, P. E., Weingartner, E.,
1024 Wex, H., Wimmer, D., Carslaw, K. S., Curtius, J., Donahue, N. M., Kirkby, J., Kulmala, M.,
1025 Worsnop, D. R., and Baltensperger, U.: Oxidation products of biogenic emissions contribute to
1026 nucleation of atmospheric particles, *Science*, 344, 717–721, doi: 10.1126/science.1243527,
1027 2014.
1028
1029 Simon, M., Heinritzi, M., Herzog, S., Leiminger, M., Bianchi, F., Praplan, A., Dommen, J.,
1030 Curtius, J., and Kürten, A.: Detection of dimethylamine in the low pptv range using nitrate
1031 chemical ionization atmospheric pressure interface time-of-flight (CI-APi-TOF) mass
1032 spectrometry, *Atmos. Meas. Tech.*, 9, 2135–2145, doi: 10.5194/amt-9-2135-2016, 2016.
1033
1034 Sipilä, M., Sarnela, N., Jokinen, T., Junninen, H., Hakala, J., Rissanen, M. P., Praplan, A.,
1035 Simon, M., Kürten, A.,, Curtius, J., Petäjä, T., and Worsnop, D. R.: Bisulfate – cluster based
1036 atmospheric pressure chemical ionization mass spectrometer for high-sensitivity (< 100 ppqV)

detection of atmospheric dimethyl amine: proof-of-concept and first ambient data from boreal forest, *Atmos. Meas. Tech.*, 8, 4001–4011, doi: 10.5194/amt-8-4001-2015, 2015.

Voigtländer, J., Duplissy, J., Rondo, L., Kürten, A., and Stratmann, F.: Numerical simulations of mixing conditions and aerosol dynamics in the CERN CLOUD chamber, *Atmos. Chem. Phys.*, 12, 2205–2214, doi: 10.5194/acp-12-2205-2012, 2012.

Wang, S. C., and Flagan, R. C.: Scanning electrical mobility spectrometer, *Aerosol Sci. Technol.*, 13, 230–240, doi: 10.1080/02786829008959441, 1990.

Weber, R. J., Marti, J., McMurry, P. H., Eisele, F. L., Tanner, D. J., and Jefferson, A.: Measured atmospheric new particle formation rates: implications for nucleation mechanisms, *Chem. Eng. Comm.*, 151, 53–64, doi: 10.1080/00986449608936541, 1996.

Weber, R. J., Marti, J. J., McMurry, P. H., Eisele, F. L., Tanner, D. J., and Jefferson, A.: Measurements of new particle formation and ultrafine particle growth rates at a clean continental site, *J. Geophys. Res.-Atmos.*, 102, D4, 4375–4385, doi: 10.1029/96JD03656, 1997.

Weber, R. J., McMurry, P. H., Mauldin, L., Tanner, D. J., Eisele, F. L., Brechtel, F. J., Kreidenweis, S. M., Kok, G. L., Schillawski, R. D., and Baumgardner, D.: A study of new particle formation and growth involving biogenic and trace gas species measured during ACE 1, *J. Geophys. Res.-Atmos.*, 103, D13, 16385–16396, doi: 10.1029/97JD02465, 1998.

Yao, L., Wang, M.-Y., Wang, X.-K., Liu, Y.-J., Chen, H.-F., Zheng, J., Nie, W., Ding, A.-J., Geng, F.-H., Wang, D.-F., Chen, J.-M., Worsnop, D. R., and Wang, L.: Detection of atmospheric gaseous amines and amides by a high-resolution time-of-flight chemical ionization mass spectrometer with protonated ethanol reagent ions, *Atmos. Chem. Phys.*, 16, 14527–14543, doi: 10.5194/acp-16-14527-2016, 2016

Zhao, J., Smith, J. N., Eisele, F. L., Chen, M., Kuang, C., and McMurry, P. H.: Observation of neutral sulfuric acid-amine containing clusters in laboratory and ambient measurements, *Atmos. Chem. Phys.*, 11, 10823–10836, doi: 10.5194/acp-11-10823-2011, 2011.

Atmos. Chem. Phys. Discuss., https://doi.org/10.5194/acp-2017-636
Manuscript under review for journal Atmos. Chem. Phys.
Discussion started: 8 August 2017

Atmospheric Chemistry and Physics Discussions

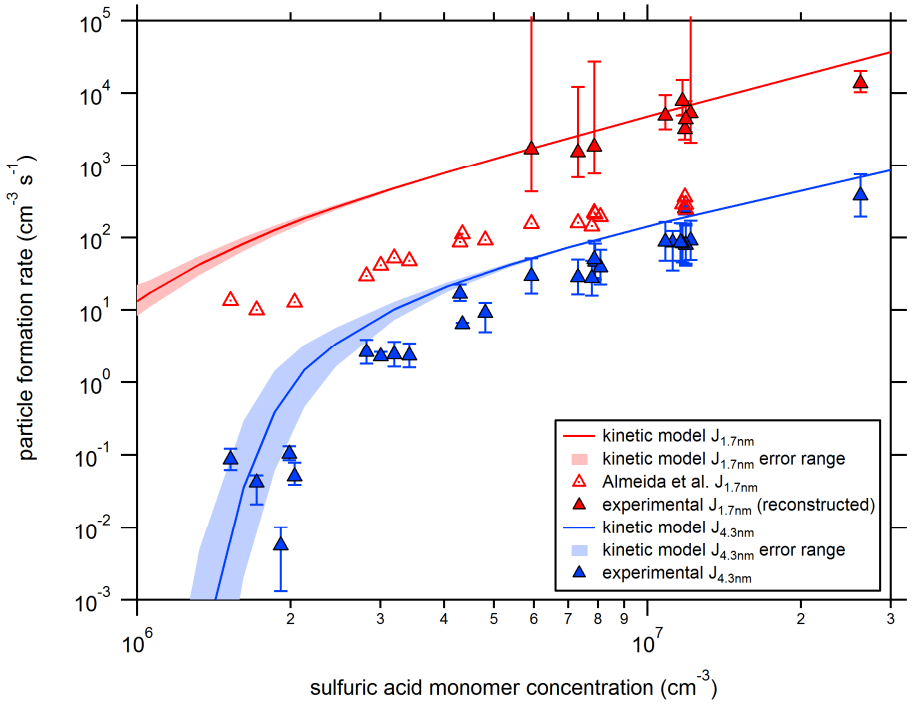

Fig. 1. Comparison between experimental and theoretical particle formation rates at two different sizes (mobility diameters of 1.7 nm and 4.3 nm). The lines indicate calculated particle formation rates from the collision-controlled aerosol model described in section 2.4 for CLOUD chamber conditions. The shaded regions show the model uncertainties when using an error of ±20% for the wall loss coefficient (C_w, see equation (2)). The open red symbols show previously published CLOUD7 data for the sulfuric acid-dimethylamine-water system (Almeida et al., 2013), while the blue symbols show the rates derived from SMPS size distribution measurements (this study). The data shown by the closed red symbols were derived with the method introduced by Kürten et al. (2015a) by extrapolating the SMPS data starting at 4.3 nm.

Atmos. Chem. Phys. Discuss., https://doi.org/10.5194/acp-2017-636
Manuscript under review for journal Atmos. Chem. Phys.
Discussion started: 8 August 2017

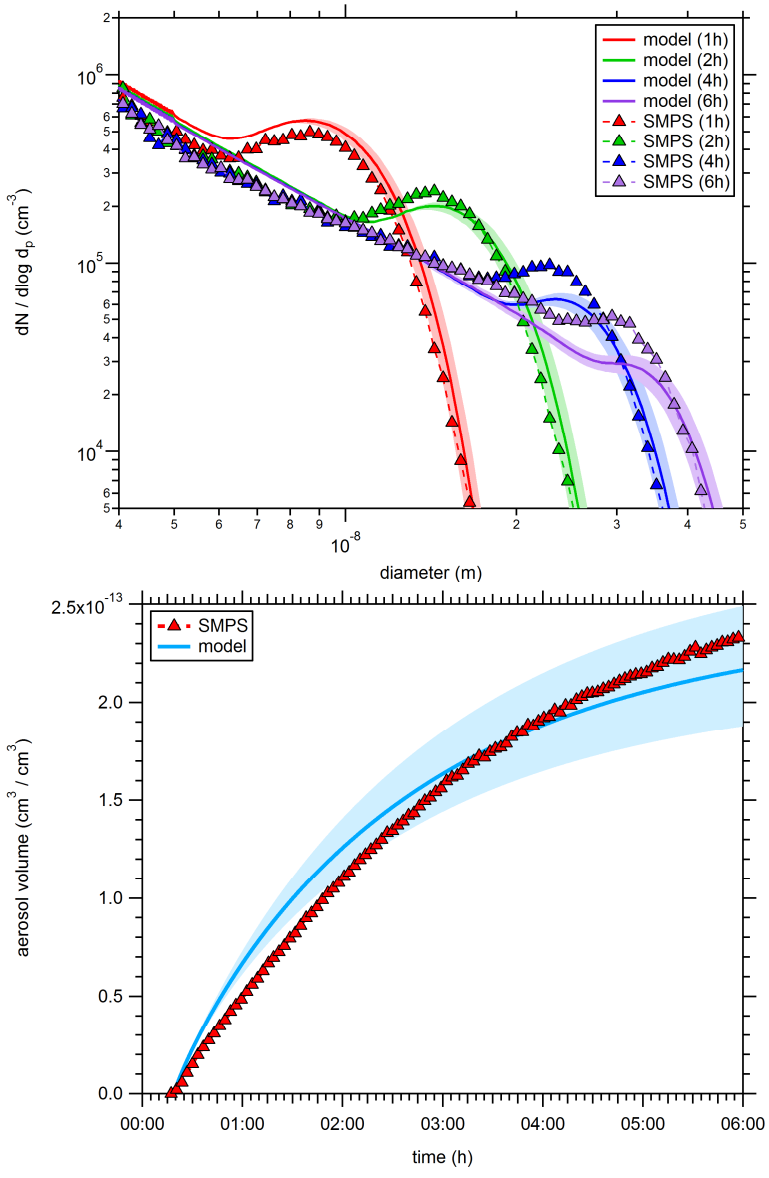

Fig. 2. Comparison between simulated and measured particle size distributions for one experiment (CLOUD7, run 1036.01). The comparison is shown in the upper panel for four different times (1h, 2h, 4h and 6h) after the start of the experiment. The lower panel shows a comparison between modeled and measured aerosol volume as a function of time. The shaded regions show the model uncertainties when using an error of ±20% for the wall loss coefficient (C_w, see equation (2)).

Atmos. Chem. Phys. Discuss., https://doi.org/10.5194/acp-2017-636
Manuscript under review for journal Atmos. Chem. Phys.
Discussion started: 8 August 2017

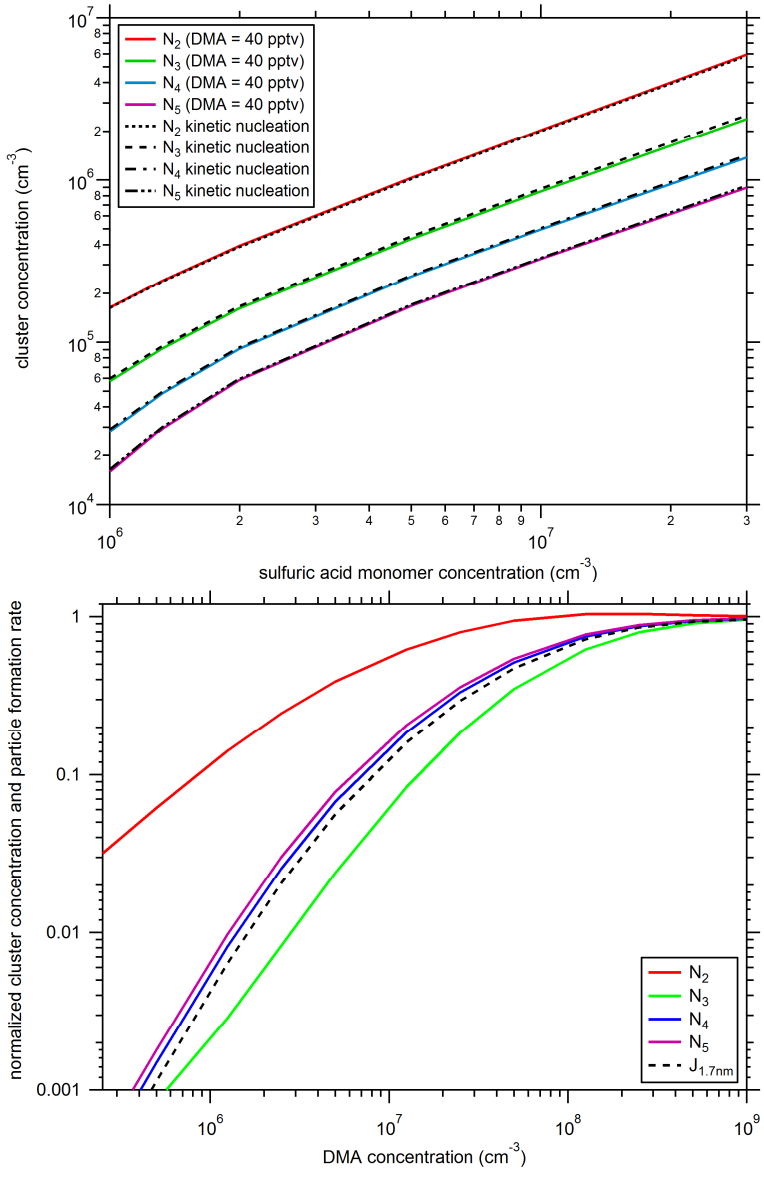

Fig. 3. Upper panel: Comparison of modeled cluster (N_2 = dimer, N_3 = trimer, N_4 = tetramer and N_5 = pentamer) concentrations using different scenarios. The dashed black lines use the collision-controlled nucleation scheme with all evaporation rates set to zero (section 2.4); while the colored solid lines are calculated based on the model by Jen et al. (2016a) with a dimethylamine mixing ratio of 40 pptv, which was the average mixing ratio during the CLOUD7 campaign. Lower panel: Variation in modeled cluster concentration and $J_{1.7nm}$ as a function of the dimethylamine mixing ratio (Jen et al., 2016a). The data were normalized to the values from the collision-controlled limit calculation (upper panel). For the calculations a sulfuric acid concentration of 5×10^6 cm^{-3} was used. See text for further details.

Atmos. Chem. Phys. Discuss., https://doi.org/10.5194/acp-2017-636
Manuscript under review for journal Atmos. Chem. Phys.
Discussion started: 8 August 2017

Atmospheric Chemistry and Physics Discussions

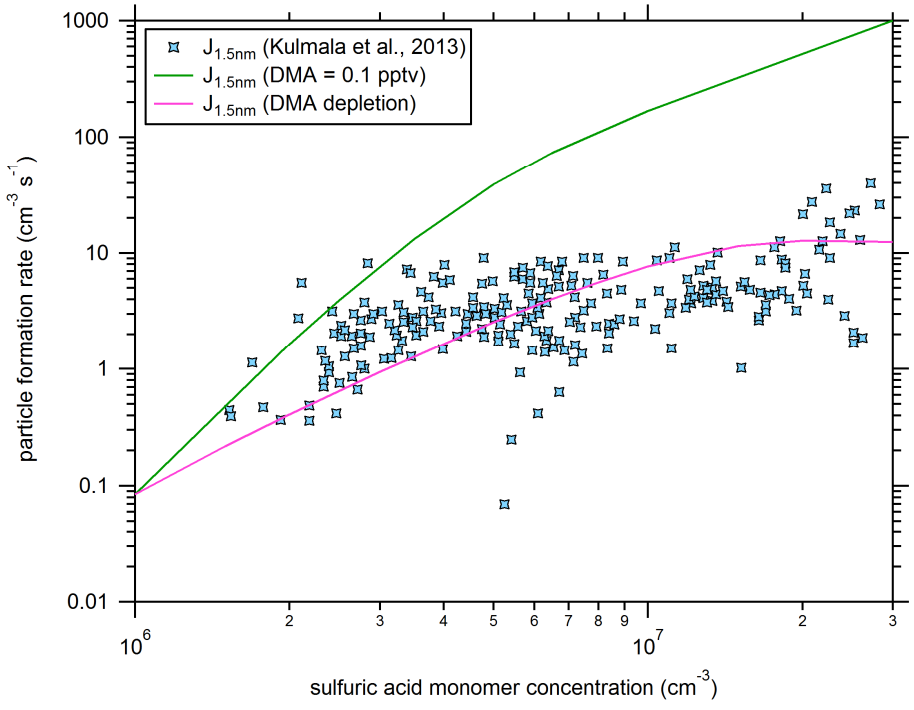

Fig. 4. Comparison between atmospheric (symbols, see Kulmala et al., 2013) and modeled new particle formation rates at 1.5 nm using the model according to Jen et al. (2016a). Using a DMA mixing ratio of 0.1 pptv results in some overlap between the atmospheric data and the modeled NPF rates (solid green line). Assuming that the DMA is depleted linearly with increasing acid concentration (starting at 0.1 pptv at 1×10^6 cm^{-3} of sulfuric acid) results in the solid magenta curve. The condensation sink (CS) in these calculations is 2×10^{-3} s^{-1}.